

## Umbilic points on Gaussian random surfaces

M V Berry† and J H Hannay‡

† H H Wills Physics Laboratory, University of Bristol, Tyndall Avenue, Bristol BS8 1TL, UK

‡ Cavendish Laboratory, Madingley Road, Cambridge CB3 0HE, UK

Received 12 May 1977, in final form 7 July 1977

**Abstract.** An umbilic point  $U$  on a surface  $\Sigma$  is a place where the two principal curvatures of  $\Sigma$  are equal.  $U$  is a singularity of  $\Sigma$  in three different senses: (i) it is the source of elliptic (E) or hyperbolic (H) umbilic catastrophes in the envelope of normals ('focal surface') of  $\Sigma$ ; (ii) it has index  $\pm\frac{1}{2}$  depending on whether the principal curvature directions of  $\Sigma$  (defining the lines of curvature) rotate by  $\pm\pi$  during a circuit of  $U$ ; (iii) it has a pattern of the 'star' (S), 'lemon' (L) or 'monstar' (M) type depending on the configuration of lines of curvature near  $U$ . We calculate the average density of umbilic points, and the fractions  $\alpha$  of umbilics of the different sorts, for the case where  $\Sigma$  is a surface whose (small) deviation from a plane is specified by a Gaussian random function. It is always the case that  $\alpha_S = \alpha_{\pm 1/2} = \frac{1}{2}$ . The other fractions depend on the degree of isotropy of the statistics of  $\Sigma$ . In the isotropic case the elliptic umbilic fraction is  $\alpha_E = 1 - \alpha_H = 0.268$ , and the monstar fraction is  $\alpha_M = \frac{1}{2} - \alpha_L = 0.053$ .

### 1. Introduction

As well as being mathematically interesting in its own right the differential geometry of curved surfaces is important in a number of physical problems. This paper is about the classification and statistics of the simplest singular points on a surface  $\Sigma$  that do not depend on the orientation of  $\Sigma$  in space. These are the 'umbilic points', defined as places where the two principal curvatures of  $\Sigma$  are equal. In optics  $\Sigma$  might be a smooth wavefront produced for example by transmission of a plane wave through an irregular refracting medium or reflection from an undulating surface. Then the normals to  $\Sigma$  are the rays of geometrical optics; the rays through umbilic points on  $\Sigma$  pass through the singular 'anastigmatic points' of the 'focal surface' that consists of the envelope of all the rays. It is near these focal points that the wave attains its greatest intensity (Berry 1976). In two-dimensional elasticity or flow  $\Sigma$  might be the graph of a smooth function of two variables whose second derivatives define a tensor field such as stress, strain or strain rate. Then umbilic points are places where the orthogonal net of principal directions of the tensor field has a singularity (Jessop and Harris 1949). Sometimes umbilic points are referred to as 'isotropic points'.

Let the umbilic point be denoted by  $U$ . Sufficiently close to  $U$ ,  $\Sigma$  is spherical by definition and can be described by its deviation  $f(\mathbf{r})$  from the tangent plane  $\mathbf{r} = (x, y)$  at  $U$  as follows:

$$f(\mathbf{r}) = \frac{1}{2}k(x^2 + y^2) + \frac{1}{6}(\alpha x^3 + 3\beta x^2 y + 3\gamma xy^2 + \delta y^3) + O(4). \quad (1)$$

Considered as a singularity of  $\Sigma$ ,  $U$  can be classified in several different ways that depend on the coefficients  $\alpha$ ,  $\beta$ ,  $\gamma$ ,  $\delta$  of the cubic terms. Thus  $U$  may be elliptic (E) or

hyperbolic (H) according to which of two possible focal surfaces is formed by the envelope of normals to  $\Sigma$  near U. This distinction is based on the catastrophe classification of Thom (1975). Alternatively U may have 'index'  $+\frac{1}{2}$  or  $-\frac{1}{2}$  depending on whether the local cross formed by the principal axes of curvature of  $\Sigma$  rotates through  $+\pi$  or  $-\pi$  in a circuit of U. Finally U may be classified by whether the orthogonal net of lines of curvature formed by the principal axes in its neighbourhood has what we call the 'star' (S), 'lemon' (L) or 'monstar' (M) pattern. The singularities E, H,  $\pm\frac{1}{2}$  and S, L, M are 'generic' (i.e. typical): no other types can occur except for umbilics belonging to a set whose measure is zero in the space  $\alpha, \beta, \gamma, \delta$ . In § 2 these classifications and the way they interlock will be summarised as a necessary basis for what follows even though the different types of umbilic have been partially described in classic works by Darboux (1896) and Gullstrand (1905) (see also Forsyth 1912), and fully described more recently by Porteous (1971).

In the important class of *Gaussian random surfaces* (which possess only generic umbilic points)  $\Sigma$  is described by its (small) undulating deviation  $h(\mathbf{r})$  from a plane  $\mathbf{r} (= (x, y))$ . Many statistical properties of such surfaces were worked out by Longuet-Higgins (1956). Infinite in extent, they have infinitely many umbilic points and in §§ 3 and 4 the average umbilic density is calculated together with the fractions  $\alpha_E, \alpha_H, \alpha_{\pm 1/2}, \alpha_S, \alpha_L, \alpha_M$  of the different sorts. It is always the case that  $\alpha_S = \alpha_{+1/2} = \alpha_{-1/2} = \frac{1}{2}$ . However, the other quantities depend on the degree of isotropy of the randomness of  $\Sigma$  (§ 5). For isotropic disorder  $\alpha_E = 1 - \alpha_H = 0.268$  while  $\alpha_M = \frac{1}{2} - \alpha_L = 0.053$ . The main results of the paper are summarised in figure 2.

## 2. Classification

The umbilic U is to be classified in three ways according to the sign of three different combinations of the coefficients  $\alpha, \beta, \gamma, \delta$  of the cubic terms in (1). These discriminants describe the local behaviour of the two principal curvatures of  $\Sigma$ . They are also related to more accessible features of the local topography; this is most conveniently described by isolating the cubic part of (1) and writing it as a function of polar angle  $\chi$  for a fixed radius  $R = (x^2 + y^2)^{1/2}$ :

$$f_c(\chi) = \frac{1}{6}R^3(\alpha \cos^3 \chi + 3\beta \cos^2 \chi \sin \chi + 3\gamma \cos \chi \sin^2 \chi + \delta \sin^3 \chi). \quad (2)$$

This is an antisymmetric function of  $\chi$  in the sense that  $f_c(\chi + \pi) = -f_c(\chi)$ . It has either a single maximum opposite a single minimum or three maxima opposite three minima depending on whether the equation  $df_c/d\chi = 0$  has two real roots or six. The number of zeros of  $f_c(\chi)$  itself will also be important. Clearly if  $df_c/d\chi$  has two zeros,  $f_c$  will also have two; otherwise it may have either two or six.

On the *catastrophe* classification U is elliptic or hyperbolic according to the behaviour of the *contours* of constant principal curvature near U. Either both principal curvatures have elliptical contours or both have hyperbolic ones. It can be shown that in the former case  $f_c(\chi)$  has six zeros, in the latter, two. The criterion therefore involves the discriminant of the cubic equation

$$\alpha t^3 + 3\beta t^2 + 3\gamma t + \delta = 0, \quad (3)$$

namely:

$$\text{if } C(\alpha, \beta, \gamma, \delta) \equiv 4(\alpha\gamma - \beta^2)(\beta\delta - \gamma^2) - (\alpha\delta - \beta\gamma)^2 \begin{cases} > 0 \\ < 0 \end{cases} \quad \begin{array}{l} \text{then E} \\ \text{then H.} \end{array} \quad (4)$$

On the *pattern* classification U falls into one of three categories depending on the local behaviour of the principal axes of curvature which generate an orthogonal net of lines of curvature over  $\Sigma$ . Near U the configuration of the net is of one of the three types illustrated in figure 1. The criterion distinguishing S from L and M is that

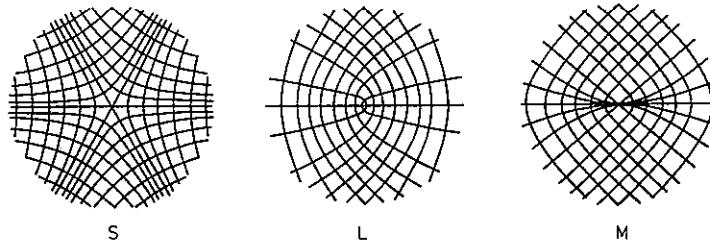


Figure 1. Lines of curvature near umbilic points with star (S), lemon (L) and monstar (M) character.

described under the index classification below. The feature distinguishing L from S and M is the number of straight lines passing through U; respectively one and three. The directions of these lines can be shown to be exactly those in which  $df_c/d\chi = 0$ . The criterion therefore involves the discriminant of the cubic equation

$$\beta t^3 + (2\gamma - \alpha)t^2 - (2\beta - \delta)t - \gamma = 0, \tag{5}$$

namely:

if  $P(\alpha, \beta, \gamma, \delta)$

$$\begin{aligned} &\equiv 4[3\gamma(\alpha - 2\gamma) - (\delta - 2\beta)^2][3\beta(\delta - 2\beta) - (\alpha - 2\gamma)^2] \\ &\quad - [(\delta - 2\beta)(\alpha - 2\gamma) - 9\beta\gamma]^2 \begin{cases} > 0 & \text{then M or S} \\ < 0 & \text{then L.} \end{cases} \end{aligned} \tag{6}$$

On the *index* classification U has index  $+\frac{1}{2}$  or  $-\frac{1}{2}$  depending again on the behaviour of the principal axes of curvature near U. In one complete circuit of U the axes rotate through half a revolution, rotating either in the same sense as the circuit executed (index  $+\frac{1}{2}$ ) or in the opposite one (index  $-\frac{1}{2}$ ). As is clear from figure 1, umbilics with L or M character have index  $+\frac{1}{2}$  while S umbilics have index  $-\frac{1}{2}$ . To derive the relevant criterion the index can be expressed as

$$\frac{1}{2\pi} \oint \nabla\theta(\mathbf{r}) \cdot d\mathbf{r} \tag{7}$$

where the integral is over an anticlockwise circuit of U and where  $\theta(\mathbf{r})$  is the angle through which the coordinate axes would have to be rotated to align them with the local principal axes. This angle is given by

$$\tan 2\theta(\mathbf{r}) = \frac{2f_{xy}(\mathbf{r})}{f_{xx}(\mathbf{r}) - f_{yy}(\mathbf{r})} = \frac{2(\beta x + \gamma y)}{(\alpha - \gamma)x + (\beta - \delta)y}. \tag{8}$$

Then after a contour integration (7) yields the following index criterion:

$$\text{if } J(\alpha, \beta, \gamma, \delta) \equiv \alpha\gamma - \gamma^2 + \beta\delta - \beta^2 \begin{cases} > 0 & \text{then index } +\frac{1}{2} \text{ (L or M)} \\ < 0 & \text{then index } -\frac{1}{2} \text{ (S).} \end{cases} \tag{9}$$

In terms of the cubic  $f_c(\chi)$ , the condition  $J = 0$  corresponds to having six zeros with four of them spaced at right angles. For if  $t (= \cot \chi)$  is a solution of (5), and so too is  $-t^{-1} (= \cot(\chi + \frac{1}{2}\pi))$ , then the third root is  $-\gamma/\beta$ , which on substitution yields  $J = 0$ . With  $J < 0$  the angular spacing between adjacent roots is acute (star), while if  $J > 0$  not all spacings are acute (monstar).

The interrelationship between the three separate classifications of umbilics can now be established. That between pattern and index classifications has already been described. Elementary manipulation of (4) and (9) shows that  $C < 0$  if  $J > 0$  so that all umbilics of index  $+\frac{1}{2}$  (i.e. lemons or monstars) must be hyperbolic in character: there exist no elliptic lemons or monstars. This means that the Venn diagram (see figure 2 and the instructive diagram on p 557 of Porteous 1971) depicting the interrelationship is effectively one dimensional.

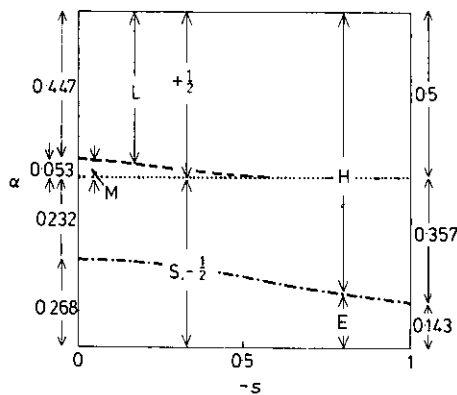


Figure 2. Venn diagram showing the interrelation between the three classifications of umbilic points and the variation of the fractions  $\alpha$  in each class with anisotropy  $s$ . The dotted line is  $J = 0$ , the broken curve  $P = 0$  and the chain curve  $C = 0$ .

### 3. Random surfaces

Consider a smooth undulating surface  $\Sigma$  specified by its deviation  $h(\mathbf{r})$  from the reference plane  $\mathbf{r} = (x, y)$ . Let  $h(\mathbf{r})$  be sufficiently small that  $(\nabla h)^2 = h_x^2 + h_y^2 \ll 1$  everywhere and employ the following symbols for the second and third derivatives:

$$\begin{aligned} h_{xx}(\mathbf{r}) &= u(\mathbf{r}), & h_{yy} &= v, & h_{xy} &= w \\ h_{xxx} &= \alpha, & h_{xxy} &= \beta, & h_{xyy} &= \gamma, & h_{yyy} &= \delta. \end{aligned} \tag{10}$$

The umbilics occur where  $u(\mathbf{r}) = v(\mathbf{r})$  and  $w(\mathbf{r}) = 0$ . The number  $N$  of umbilics on any area  $A$  of  $\Sigma$  is therefore

$$N = \iint_A dx dy \delta(u(\mathbf{r}) - v(\mathbf{r})) \delta(w(\mathbf{r})) \left| \det \frac{\partial(u - v, w)}{\partial(x, y)} \right|, \tag{11}$$

where  $\delta$  here denotes the Dirac delta function. The Jacobian determinant here is precisely  $J(\alpha, \beta, \gamma, \delta)$  defined in (9).

Now let  $h(\mathbf{r})$  be a stationary random function. Then if ensemble averages are denoted by overbars the mean number  $n$  of umbilic points per unit area is, from (11),

$$n = \overline{\delta(u-v)\delta(w)|J(\alpha, \beta, \gamma, \delta)|}. \tag{12}$$

The mean number of umbilics of any particular type can be expressed with the aid of the discriminating functions of § 2 and the unit step function  $H(X)$ . Division by  $n$  gives the fraction of umbilics of each type. Thus

$$\alpha_{-1/2} = 1 - \alpha_{+1/2} = \alpha_S = \overline{\delta(u-v)\delta(w)(-J(\alpha, \beta, \gamma, \delta))H(-J(\alpha, \beta, \gamma, \delta))}/n \tag{13}$$

$$\alpha_E = 1 - \alpha_H = \overline{\delta(u-v)\delta(w)(-J(\alpha, \beta, \gamma, \delta))H(C(\alpha, \beta, \gamma, \delta))}/n \tag{14}$$

$$\alpha_L = 1 - \alpha_S - \alpha_M = \overline{\delta(u-v)\delta(w)(J(\alpha, \beta, \gamma, \delta))H(-P(\alpha, \beta, \gamma, \delta))}/n. \tag{15}$$

The omission of the modulus signs which will greatly simplify subsequent calculations is justified by the derived interrelationship of  $J$ ,  $C$  and  $P$  (figure 2 and its caption).

To evaluate the averages in (12) to (15) it is necessary to supply the statistics of the stationary random function  $h(\mathbf{r})$ ; specifically the joint probability distribution of  $u, v, w, \alpha, \beta, \gamma, \delta$  is required. The statistics to be supplied are those of a *Gaussian* random function. It is well known (see for example Longuet-Higgins 1956) that such functions form an ensemble, each member of which is a superposition of infinitely many sinusoidal components with random phases. The 'power spectrum'  $E(\mathbf{k})$  which specifies the relative strength of the components with wavevector  $\mathbf{k} \equiv (k_x, k_y)$  bears a Fourier transform relationship to the autocorrelation function  $\rho(\mathbf{r})$  of  $h(\mathbf{r})$ :

$$\rho(\mathbf{r}) \equiv \overline{h(\mathbf{r}_0)h(\mathbf{r}_0 + \mathbf{r})} = \int d^2k e^{i\mathbf{k}\cdot\mathbf{r}} E(\mathbf{k}). \tag{16}$$

Either one of these functions completely defines the statistics of  $h(\mathbf{r})$  as follows.

By virtue of the random phase property, the joint probability distribution of any set of quantities  $\{\xi_1, \xi_2, \xi_3, \dots, \xi_n\}$  linear in  $h$  (e.g. the values of  $h$  at different points) is joint Gaussian:

$$P(\xi_1, \xi_2, \dots, \xi_n) = \frac{1}{(2\pi)^{n/2} [\det(\Xi^{-1})]^{1/2}} \exp[-\frac{1}{2}(\Xi^{-1})_{ij}\xi_i\xi_j], \tag{17}$$

where  $\Xi^{-1}$  is the inverse of the matrix of correlations

$$\Xi = \overline{\xi_i\xi_j}, \tag{18}$$

which is directly related to the autocorrelation function  $\rho$ .

If the  $\xi$  are taken to be derivatives of  $h$  evaluated at the same place, the mean product of any two of them is given by

$$\frac{\partial^{p+q}h}{\partial x^p \partial y^q} \frac{\partial^{p'+q'}h}{\partial x^{p'} \partial y^{q'}} = \frac{\partial^{p+q+p'+q'}}{\partial x^{p+p'} \partial y^{q+q'}} \rho(\mathbf{0}) \tag{19}$$

$$= (-1)^{\frac{1}{2}(p+p'+q+q')} m_{p+p', q+q'}, \tag{20}$$

where

$$m_{rs} = \int d^2k k_x^r k_y^s E(\mathbf{k}). \tag{21}$$

It follows from the symmetry of  $\rho(\mathbf{r})$  and therefore of  $E(\mathbf{k})$  that  $m_{rs}$  is zero for  $r+s$  odd. Any odd derivative of  $h$  is therefore uncorrelated with any even one, which for a joint Gaussian distribution (17) means that odd and even derivatives are statistically

independent. This applies in particular to the second and third derivatives (10) with the result that the average in (12) factorises into two separate averages over  $u, v, w$  and  $\alpha, \beta, \gamma, \delta$ , while in (13) to (15) the averages involving  $u, v, w$  cancel.

#### 4. Isotropic disorder

In this case the autocorrelation function  $\rho$  depends only on the distance  $r$  between  $\mathbf{r}_0$  and  $\mathbf{r}_0 + \mathbf{r}$  and the power spectrum  $E$  depends only on  $k \equiv |\mathbf{k}|$ . The moments  $m_{rs}$  (21) of the power spectrum can then be written

$$m_{rs} = M_{r+s} \left( \frac{1}{2\pi} \int_0^{2\pi} \cos^r \theta \sin^s \theta \, d\theta \right) \quad (22)$$

where

$$M_n \equiv 2\pi \int_0^\infty dk k^{n+1} E(k). \quad (23)$$

It is in terms of these 'circular moments'  $M_n$  that the results will be expressed.

From (20), (22) and (23) the matrix of correlations for the second derivatives,  $\Xi_2$ , is given by

$$\Xi_2 = \begin{pmatrix} \overline{u^2} & \overline{uv} & \overline{uw} \\ \overline{vu} & \overline{v^2} & \overline{vw} \\ \overline{wu} & \overline{wv} & \overline{w^2} \end{pmatrix} = \frac{M_4}{8} \begin{pmatrix} 3 & 1 & 0 \\ 1 & 3 & 0 \\ 0 & 0 & 1 \end{pmatrix} \quad (24)$$

with inverse

$$\Xi^{-1} = \frac{1}{M_4} \begin{pmatrix} 3 & -1 & 0 \\ -1 & 3 & 0 \\ 0 & 0 & 8 \end{pmatrix}. \quad (25)$$

Taken together with (17), this means that the average over  $u, v, w$  in (12) is

$$\begin{aligned} & \overline{\delta(u-v)\delta(w)} \\ &= \frac{8}{(2\pi)^{3/2} M_4^{3/2}} \int du \int dv \int dw \delta(u-v)\delta(w) \\ & \quad \times \exp\left(-\frac{1}{2M_4}(3u^2 - 2uv + 3v^2 + 8w^2)\right) \\ &= \frac{2}{\pi M_4}. \end{aligned} \quad (26)$$

(Unless otherwise stated all integrations are from  $-\infty$  to  $+\infty$ .)

For the third derivatives the correlation matrix  $\Xi_3$  is given by

$$\Xi_3 = \begin{pmatrix} \overline{\alpha^2} & \overline{\alpha\beta} & \overline{\alpha\gamma} & \overline{\alpha\delta} \\ \overline{\beta\alpha} & \overline{\beta^2} & \overline{\beta\gamma} & \overline{\beta\delta} \\ \overline{\gamma\alpha} & \overline{\gamma\beta} & \overline{\gamma^2} & \overline{\gamma\delta} \\ \overline{\delta\alpha} & \overline{\delta\beta} & \overline{\delta\gamma} & \overline{\delta^2} \end{pmatrix} = \frac{M_6}{16} \begin{pmatrix} 5 & 0 & 1 & 0 \\ 0 & 1 & 0 & 1 \\ 1 & 0 & 1 & 0 \\ 0 & 1 & 0 & 5 \end{pmatrix} \quad (27)$$

with inverse

$$\Xi_3^{-1} = \frac{4}{M_6} \begin{pmatrix} 1 & 0 & -1 & 0 \\ 0 & 5 & 0 & -1 \\ -1 & 0 & 5 & 0 \\ 0 & -1 & 0 & 1 \end{pmatrix}. \tag{28}$$

The simplest average over  $\alpha, \beta, \gamma, \delta$  appears in (12) and is

$$\begin{aligned} \overline{|J(\alpha, \beta, \gamma, \delta)|} &= \frac{64}{(2\pi M_6)^2} \int d\alpha \int d\beta \int d\gamma \int d\delta |J(\alpha, \beta, \gamma, \delta)| \\ &\quad \times \exp\left(-\frac{2}{M_6}(\alpha^2 - 2\alpha\gamma + 5\gamma^2 + \delta^2 - 2\beta\delta + 5\beta^2)\right). \end{aligned} \tag{29}$$

Under the transformation defined by

$$\begin{aligned} \alpha - \gamma &= \frac{1}{2}(\frac{1}{2}M_6)^{1/2}(X + Y), & \delta - \beta &= \frac{1}{2}(\frac{1}{2}M_6)^{1/2}(Z + T), \\ \beta &= \frac{1}{4}(\frac{1}{2}M_6)^{1/2}(Z - T), & \gamma &= \frac{1}{4}(\frac{1}{2}M_6)^{1/2}(X - Y), \end{aligned} \tag{30}$$

this becomes

$$\begin{aligned} \overline{|J|} &= \frac{M_6}{16(2\pi)^2} \int dX \int dY \int dZ \int dT |X^2 + Z^2 - Y^2 - T^2| \\ &\quad \times \exp[-\frac{1}{2}(X^2 + Y^2 + Z^2 + T^2)]. \end{aligned} \tag{31}$$

This integration is elementary in polar coordinates

$$\begin{aligned} X &= r \cos \theta, & Z &= r \sin \theta, \\ Y &= \rho \cos \phi, & T &= \rho \sin \phi, \end{aligned} \tag{32}$$

and gives the value  $8\pi^2$ . Thus

$$\overline{|J|} = M_6/8. \tag{33}$$

With (12) and (26) the average number of umbilic points per unit area is therefore

$$n = \frac{M_6}{4\pi M_4}. \tag{34}$$

For an autocorrelation function with the Gaussian form  $\exp(-r^2/\lambda^2)$  this gives  $n = 3/\pi\lambda^2$ , while for a Lorentzian  $(1 + r^2/\lambda^2)^{-1}$ ,  $n$  is three times this value.

It is obvious from (31) that half the value of the integral comes from the region in  $X, Y, Z, T$  where the quantity between the modulus signs is positive and half from where it is negative. From (13) this implies at once that

$$\alpha_{+1/2} = \alpha_{-1/2} = \alpha_S = \frac{1}{2}. \tag{35}$$

As will be shown in § 5 this result is not restricted to isotropically disordered surfaces.

Now consider the integral involved in  $\alpha_E$  (equation (14)). This is similar to (13) but the integral contains a step function of  $C$  defined by (4). The transformations (30) and (32) give

$$\begin{aligned} & -J(\alpha, \beta, \gamma, \delta)H(C(\alpha, \beta, \gamma, \delta)) \\ &= \frac{M_6}{16(2\pi)^2} \int_0^{2\pi} d\theta \int_0^{2\pi} d\phi \int_0^\infty r dr \int_0^\infty \rho d\rho (\rho^2 - r^2) e^{-\frac{1}{2}(\rho^2 + r^2)} \\ & \quad \times H\left(-\frac{3}{4}r^4 - \frac{3}{2}r^2\rho^2 + \frac{1}{4}\rho^4 + 2r^3\rho \cos(3\theta + \phi)\right). \end{aligned} \quad (36)$$

One angular integration is trivial and the substitution

$$r = \rho u \quad (37)$$

enables the integral over  $\rho$  to be performed. After some reduction this gives

$$\alpha_E = \frac{9}{50} + \frac{8}{\pi} \int_{1/3}^1 du \frac{u(1-u^2)}{(1+u^2)^3} \sin^{-1} \left[ \left( \frac{(1-u)^3(3u+1)}{16u^3} \right)^{1/2} \right]. \quad (38)$$

A simple numerical integration then yields

$$\alpha_E = 0.268. \quad (39)$$

The expression (38) has a simple geometrical significance in terms of the cubic (2) which is described in the appendix.

The fraction  $\alpha_L$  (equation (15)) can be calculated either directly by the transformations (30), (32) and (37) used for  $\alpha_E$ , or from the geometrical argument outlined in the appendix. This shows that  $\alpha_L$  is obtained by replacing  $u$  by  $u/3$  within the square root in (38), and the  $\sin^{-1}$  by  $-\cos^{-1}$ , replacing the range of integration by 1 to 3:

$$\alpha_L = \frac{9}{50} + \frac{8}{\pi} \int_1^3 du \frac{u(u^2-1)}{(1+u^2)^3} \cos^{-1} \left[ \left( \frac{(3-u)^3(1+u)}{16u^3} \right)^{1/2} \right]. \quad (40)$$

Integrated numerically this gives

$$\alpha_L = 0.447 \quad \text{i.e.} \quad \alpha_M = 0.053. \quad (41)$$

## 5. Anisotropic disorder

If the autocorrelation function  $\rho(\mathbf{r})$  is not circularly symmetric the correlation matrices (24) and (27) will have elements depending on its detailed form. This will affect both the mean density of umbilic points  $n$  and the various fractions  $\alpha$  with the important exception of  $\alpha_{\pm 1/2}$ . It follows quite generally from the circuit definition (7) that deformations of a surface can create or destroy umbilic points only in groups for which the algebraic sum of the indices (the 'total index') is zero (generically these will be pairs with index  $+\frac{1}{2}$  and  $-\frac{1}{2}$ ). For a closed (one-sided) surface this means that the total index must be a constant, and it is not difficult to show that this constant is actually equal to the integrated Gaussian curvature of the surface divided by  $2\pi$  (i.e. to the Euler characteristic of the surface). Imagine now that the random surface  $\Sigma$  is locally part of a huge dimpled torus. Since the statistics are stationary, the vanishing of the total index over the whole torus, required by the zero integrated Gaussian curvature, implies the vanishing of the *average* total index over any part of the torus and hence

over any part of  $\Sigma$ . The result (35) for  $\alpha_{\pm 1/2}$  therefore applies to all stationary random functions, and in particular to Gaussian ones whatever form the correlation function may take. (The result need not, however, apply to random surfaces like sponges which could have integrated Gaussian curvature proportional to their surface area.)

One particularly simple form of anisotropisation will now be considered quantitatively—that made by stretching an initially isotropic surface by a factor  $\sigma$  along  $x$  and simultaneously compressing it by the same factor along  $y$ . The correlation function  $\rho$  becomes wider along  $x$  and narrower along  $y$  in exactly the same way, with the associated reciprocal effect on the spectrum  $E$ . The inverse correlation matrices corresponding to (25) and (28) are then easily found to be, respectively,

$$\frac{1}{M_4} \begin{pmatrix} 3\sigma^4 & -1 & 0 \\ -1 & 3\sigma^{-4} & 0 \\ 0 & 0 & 8 \end{pmatrix} \tag{42}$$

and

$$\frac{4}{M_6} \begin{pmatrix} \sigma^6 & 0 & -\sigma^2 & 0 \\ 0 & 5\sigma^2 & 0 & -\sigma^{-2} \\ -\sigma^2 & 0 & 5\sigma^{-2} & 0 \\ 0 & \sigma^{-2} & 0 & \sigma^{-6} \end{pmatrix}, \tag{43}$$

where the  $M$  are the circular moments of the isotropic spectrum before stretching.

In the average (26) over second derivatives, the quadratic form in the exponent, now being governed by (42), changes to  $3\sigma^4 u^2 - 2uv - 3\sigma^{-4} v^2 + 8w^2$ . In terms of the convenient 'reduced stretch'  $s$  defined by

$$S \equiv \frac{\sigma^4 - 1}{\sigma^4 + 1}, \tag{44}$$

which ranges from 0 to 1 as  $\sigma$  ranges from 1 to  $\infty$ , the integration then gives

$$\overline{\delta(u-v)\delta(w)} = \frac{4}{\pi M_4 (3\sigma^4 - 2 + 3\sigma^{-4})^{1/2}} = \frac{2}{\pi M_4} \left( \frac{1-s^2}{1+2s^2} \right)^{1/2}. \tag{45}$$

The averages over the third derivatives are less easily converted. In the simplest one (29) for  $|J|$ , the quadratic form in the exponent, now being governed by (43), changes to  $\sigma^6 \alpha^2 - 2\sigma^2 \alpha\gamma + 5\sigma^{-2} \gamma^2 + \sigma^{-6} \delta^2 - 2\sigma^{-2} \beta\delta + 5\sigma^2 \beta^2$ . To follow the isotropic calculation as closely as possible, introduce the change of variables

$$\begin{aligned} \sigma^3 \alpha - \sigma^{-1} \gamma &= \frac{1}{2} (\frac{1}{2} M_6)^{1/2} (X + Y), & \sigma^{-3} \delta - \sigma \beta &= \frac{1}{2} (\frac{1}{2} M_6)^{1/2} (Z + T), \\ \sigma \beta &= \frac{1}{4} (\frac{1}{2} M_6)^{1/2} (Z - T), & \sigma^{-1} \gamma &= \frac{1}{4} (\frac{1}{2} M_6)^{1/2} (X - Y). \end{aligned} \tag{46}$$

This gives

$$|J| = \frac{1}{(2\pi)^2} \int dX \int dY \int dZ \int dT |\mathcal{J}| \exp[-\frac{1}{2}(X^2 + Y^2 + Z^2 + T^2)] \tag{47}$$

with

$$\mathcal{J} \equiv \frac{M_6}{32} (XYZT) \begin{pmatrix} 3\sigma^{-2} - \sigma^2 & \sigma^2 - \sigma^{-2} & 0 & 0 \\ \sigma^2 - \sigma^{-2} & -\sigma^2 - \sigma^{-2} & 0 & 0 \\ 0 & 0 & 3\sigma^2 - \sigma^{-2} & \sigma^{-2} - \sigma^2 \\ 0 & 0 & \sigma^{-2} - \sigma^2 & -\sigma^2 - \sigma^{-2} \end{pmatrix} \begin{pmatrix} X \\ Y \\ Z \\ T \end{pmatrix}. \tag{48}$$

The eigenvalues of this matrix are

$$2l_1/(1-s^2)^{1/2}, \quad 2l_2/(1-s^2)^{1/2}, \quad -2l_3/(1-s^2)^{1/2}, \quad -2l_4/(1-s^2)^{1/2},$$

where the  $l$  are positive quantities which remain finite for all  $0 < s < 1$ :

$$\begin{aligned} l_1 &= s + (2s^2 + 2s + 1)^{1/2} & l_2 &= -s + (2s^2 - 2s + 1)^{1/2} \\ l_3 &= -s + (2s^2 + 2s + 1)^{1/2} & l_4 &= s + (2s^2 - 2s + 1)^{1/2}. \end{aligned} \quad (49)$$

An orthogonal change of variables to diagonalize the matrix in (48) therefore yields

$$\begin{aligned} |\overline{J}| &= \frac{M_6}{16(2\pi)^2} \frac{1}{(1-s^2)^{1/2}} \int d\xi \int d\eta \int d\zeta \int d\tau |l_1\xi^2 + l_2\eta^2 - l_3\zeta^2 - l_4\tau^2| \\ &\quad \times \exp[-\frac{1}{2}(\xi^2 + \eta^2 + \zeta^2 + \tau^2)]. \end{aligned} \quad (50)$$

The integral  $I(s)$  in this expression can be evaluated most easily by an indirect method. Two further integrations over auxiliary variables  $\mu$  and  $\nu$  are introduced to give

$$\begin{aligned} I(s) &= \frac{1}{2\pi} \int d\mu \int d\nu \int d\xi \int d\eta \int d\zeta \int d\tau |\nu| \exp[-i\mu(l_1\xi^2 + l_2\eta^2 - l_3\zeta^2 - l_4\tau^2)] \\ &\quad \times \exp[-\frac{1}{2}(\xi^2 + \eta^2 + \zeta^2 + \tau^2)] \end{aligned} \quad (51)$$

(that this expression is equivalent to (50) can be seen by performing first the  $\mu$  integral and then the  $\nu$  one). The  $\xi, \eta, \zeta, \tau$  integrations in (51) are trivial and the  $\nu$  integral (with the correct interpretation as a generalised Fourier transform) gives

$$I(s) = 2\pi \int -\frac{1}{\mu} \frac{d}{d\mu} \frac{1}{[(1-2i\mu l_1)(1-2i\mu l_2)(1+2i\mu l_3)(1+2i\mu l_4)]^{1/2}} d\mu. \quad (52)$$

The singularities of the integrand are four branch points on the imaginary axis, one pair above and another below the real axis. There is no singularity at the origin because by (49),  $l_1 + l_2 = l_3 + l_4$  so that the derivative is zero there. If branch cuts are inserted between each pair of branch points the contour of integration can be closed around either half-plane.  $I(s)$  is therefore given by either one of the two, equal, branch cut integrals. The two alternatives correspond to the evaluation of  $2JH(J)$  (upper half-plane) or  $2(-J)H(-J)$  (lower half-plane), which are therefore individually equal to  $|\overline{J}|$ . This is the statement that umbilics of index  $\pm \frac{1}{2}$  are equally likely. The (upper) branch cut integral is

$$I(s) = 4\pi \int_{1/l_3}^{1/l_4} \frac{1}{\mu^2} \frac{1}{[-(1+2\mu l_1)(1+2\mu l_2)(1-2\mu l_3)(1-2\mu l_4)]^{1/2}} d\mu, \quad (53)$$

where an integration by parts has been performed to eliminate the derivative.

This integral can be evaluated in terms of complete elliptic integrals (Byrd and Friedman 1954) but the resulting expression is very long. Instead numerical evaluation (with the trigonometric substitution  $\sin^2\theta = [\mu l_4 + (1-\mu)l_3]/2l_3l_4$ ) shows that  $I(s)$  rises monotonically from the value  $8\pi^2$  when  $s = 0$  (isotropy) to  $1.88 \times 8\pi^2$  when  $s = 1$  (extreme anisotropy). Thus

$$|\overline{J}| = \frac{M_6}{8} \frac{I(s)/8\pi^2}{(1-s^2)^{1/2}} \quad \left(1 \leq \frac{I(s)}{8\pi^2} \leq 1.88\right). \quad (54)$$

Taken together with (12) and (45) this gives

$$n = \frac{M_6}{4\pi M_4} \left( \frac{I(s)}{8\pi^2(1+2s^2)^{1/2}} \right) \quad \left( 1 \leq \frac{I(s)}{8\pi^2(1+2s^2)^{1/2}} \leq 1.08 \right), \quad (55)$$

showing that area preserving strain leaves the density of umbilic points virtually constant.

Anisotropisation does, however, markedly change the character of the umbilic points as characterised by the fractions  $\alpha_E$  and  $\alpha_L$ . A great simplification arises in the case of  $\alpha_E$  because  $C(\alpha, \beta, \gamma, \delta) = C(\sigma^3\alpha, \sigma\beta, \sigma^{-1}\gamma, \sigma^{-3}\delta)$ . This means that when, in analogy with the isotropic case, the transformations (46) and (32) are applied the resulting equation has a form identical with (36) apart from the replacement

$$\rho^2 - r^2 \rightarrow \frac{1}{(1-s^2)^{1/2}} [\rho^2 - r^2 - 2sr(\rho \cos(\theta + \phi) - r \cos 2\theta)]. \quad (56)$$

The terms involving  $\theta$  and  $\phi$  vanish on integration giving the result that the only effect of anisotropy on  $\sqrt{|J|H(C)}$  is a factor  $1/(1-s^2)^{1/2}$ . From (14), (33) and (54) therefore

$$\alpha_E = \frac{0.268}{I(s)/8\pi^2} \quad (0.268 \geq \alpha_E \geq 0.143). \quad (57)$$

In the case of  $\alpha_L$  the same simplification does not occur and there is no obvious way to evaluate  $\sqrt{|J|H(P)}$  analytically, though the behaviour of  $\alpha_L$  for extreme anisotropy can be found as follows. Construct the quantities  $\alpha' = \sigma^3\alpha$ ,  $\beta' = \sigma\beta$ ,  $\gamma' = \sigma^{-1}\gamma$ ,  $\delta' = \sigma^{-3}\delta$  so that the probability distribution for  $\alpha'$ ,  $\beta'$ ,  $\gamma'$ ,  $\delta'$  is independent of  $\sigma$ . In terms of these well behaved quantities, as  $\sigma \rightarrow \infty$

$$\begin{aligned} J &\rightarrow \sigma^2(\beta'\delta' - \gamma'^2) \\ P &\rightarrow \sigma^8\delta^2(\gamma'^2 - \beta'\delta'). \end{aligned} \quad (58)$$

Therefore for extreme anisotropy  $P$  is always negative with  $J$  is positive so that all umbilics with index  $+\frac{1}{2}$  are lemons; *there are no monstars*:

$$\alpha_L = \frac{1}{2}, \quad \alpha_M = 0. \quad (59)$$

The behaviour of  $\alpha_L$  for intermediate degrees of anisotropy shown in figure 2 was obtained by direct Monte Carlo numerical evaluation of  $\sqrt{|J|H(P)}/|J|$ .

## 6. Conclusion

The classification of umbilic points in figure 2 illustrates the fact that the same geometric object can be a singularity in several different senses; it would be a mistake to assume that any one of the classifications of singularity (e.g. catastrophes) is necessarily more fundamental than the others. The index classification, for example, can provide important information on the global characteristics of the focal pattern beyond an illuminated irregular diffracting screen, in contrast to the local information provided by the catastrophe classification.

The main results of our 'statistical singularity theory' are summarised in figure 2. The most striking conclusion is the rarity of monstar patterns and to a lesser extent elliptic umbilic catastrophes. It is tempting to think that this explains the difficulties experienced by Thom and Poston (private communications) in producing elliptic

umbilics by optical means. Any such argument would depend on Gaussian random surfaces being representative of other irregular surfaces. But it is not difficult to create a whole class of surfaces whose umbilics must all be elliptic. These surfaces (which do not contravene the index laws because they cannot be closed and can depart little from a plane only locally) are those of liquids in equilibrium under surface tension at uniform pressure (e.g. small water drops on a dirty solid surface). It is plausible though that such surfaces are the exception rather than the rule in the entirety of irregular surfaces that nature generates.

### Acknowledgments

We thank Mr P F Miller and Professor J F Nye for many helpful discussions.

### Appendix. Geometrical interpretation of the integrals for isotropic disorder

The function cubic  $f_c(\chi)$ , defined as (2), describing the behaviour of the surface  $\Sigma$  in the neighbourhood of an umbilic point can be re-expressed as the real part of a complex function of  $\alpha, \beta, \gamma, \delta$  as follows

$$\begin{aligned} f_c(\chi) &= \frac{1}{24}R^3[(\alpha - 3\gamma) \cos 3\chi - (\delta - 3\beta) \sin 3\chi + 3(\alpha + \gamma) \cos \chi + 3(\beta + \delta) \sin \chi] \\ &= \frac{1}{24}R^3 \operatorname{Re}(r e^{i(\chi - \theta)} + \rho e^{i(3\chi + \phi)}) \end{aligned} \quad (\text{A.1})$$

where the variables  $r, \rho, \theta, \phi$  are exactly those defined in (32). As the angle  $\chi$  increases from 0 to  $2\pi$  the complex number in (A.1) traces out a symmetrical figure in the Argand diagram generated by the sum of two 'vectors' one rotating three times as fast as the other. The orientation of the figure will depend on the angles  $\theta$  and  $\phi$  but its shape depends only on the ratio  $3u (= 3r/\rho)$  of the lengths of the two vectors. There are four distinct regimes of  $u$  which produce the shapes shown at the bottom of figure 3. For a figure with a given shape and orientation the following rules, easily verified from § 2, serve to identify the status of the umbilic;

$J > 0$ ( $\equiv$ index $+\frac{1}{2}$ )	figure has loops
$J < 0$ ( $\equiv$ index $-\frac{1}{2}$ )	figure has no loops
$C > 0$ ( $\equiv$ elliptic)	figure intersects imaginary axis six times
$C < 0$ ( $\equiv$ hyperbolic)	figure intersects imaginary axis twice
$P > 0$ ( $\equiv$ not lemon)	figure tangent lies parallel to imaginary axis six times
$P < 0$ ( $\equiv$ lemon)	figure tangent lies parallel to imaginary axis twice.

From these rules it can be seen by referring to figure 3 that there are no elliptic umbilics for  $u > 1$ , while for  $u < \frac{1}{3}$  all umbilics are elliptic. For intermediate values of  $u$  the umbilic may or may not be elliptic depending on the orientation of the figure. Similarly there are no lemon umbilics for  $u < 1$ , while for  $u > 3$  all umbilics are lemon. In between, an umbilic may be lemon or not according to the figure orientation.

It is now possible to interpret the integrals (38) and (40) in a rather simple way. For an isotropically disordered surface it follows from (32) that the complex numbers  $re^{i\theta}$  and  $\rho e^{i\phi}$  have identical, independent, circular Gaussian distributions in the Argand

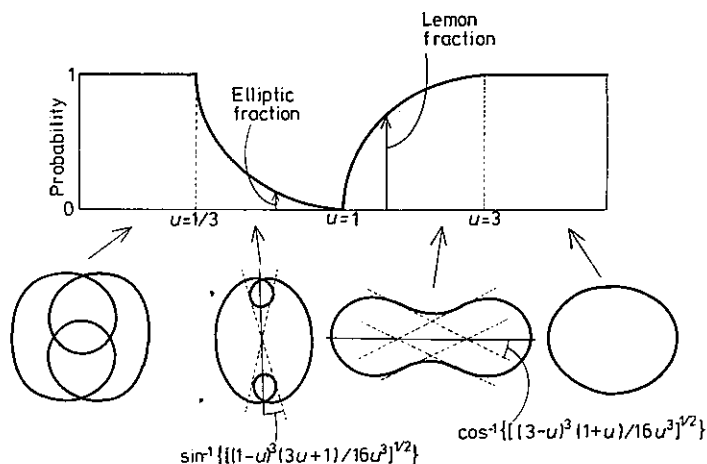


**Figure 3.** Representation of the cubic expansion near an umbilic point by figures in the Argand diagram, generated by the resultant of three rotating vectors, one turning three times as fast as the other. The ratio  $u$  of the lengths of these vectors determines the shape of each figure and the resulting sector angles determine the chance that the umbilic is elliptic (for  $u < 1$ ) and lemon (for  $u > 1$ ).

diagram. This means that a figure of any given shape determined by the ratio  $u$  is *equally likely* to be found in any orientation. The angles appearing in (38) and (40) are just the sector angles marked in figure 3, which when divided by  $\pi/2$  give the probability that the figure represents an elliptic umbilic in the first case and a lemon umbilic in the second. The factor  $4u|1-u^2|/(1+u^2)^3$  in each integral is the probability distribution for the ratio  $u$ , taking into account the Jacobian weighting factor  $|\rho^2-r^2|$ . When this function is integrated from 0 to  $\frac{1}{3}$  it gives the same answer as when integrated from 3 to  $\infty$ , namely  $9/50$ .

## References

- Berry M V 1976 *Adv. Phys.* **25** 1–26  
 Byrd P F and Friedman M D 1954 *Elliptic Integrals for Scientists and Engineers* (Berlin: Springer)  
 Darboux G 1896 *Leçons sur la Théorie Générale des Surfaces* vol. 4 (Paris: Gauthier-Villars) note VII  
 Forsyth A R 1912 *Differential Geometry* (Cambridge: Cambridge University Press) chap. 4  
 Gullstrand A 1905 *Acta Math.* **29** 59–100  
 Jessop H T and Harris F C 1949 *Photoelasticity* (London: Cleaver-Hume)  
 Longuet-Higgins M S 1956 *Phil. Trans. R. Soc. A* **249** 321–87  
 Porteous I R 1971 *J. Diff. Geom.* **5** 543–64  
 Thom R 1975 *Structural Stability and Morphogenesis* (Reading, Mass.: Benjamin)